Experimental Eye Research 263 (2026) 110775

Contents lists available at ScienceDirect

Experimental Eye Research

journal homepage: www.elsevier.com/locate/yexer

Research article

Regenerative effects of topical insulin on corneal wound healing: From surface restoration to stromal remodeling

Yurdagul Girgin [a], Gozde Sahin Vural [b,*], Yucel Yigit [c], Basak Isildar [d], Pakize Nur Akkaya [d], Gamze Tanriverdi [e], Muhammed Dara Tas [f], Ozlem Barut Selver [f,g,h,i,j]

[a] Corlu State Hospital, Department of Ophthalmology, Tekirdag, Turkey
[b] Balıkesir University, Faculty of Medicine, Department of Ophthalmology, Balikesir, Turkey
[c] Arnavutkoy State Hospital, Department of Ophthalmology, Istanbul, Turkey
[d] Balikesir University, Department of Histology and Embryology, Balikesir, Turkey
[e] Istanbul University-Cerrahpasa, Department of Histology and Embryology, Istanbul, Turkey
[f] Ege University, Faculty of Medicine, Department of Ophthalmology, Izmir, Turkey
[g] Ege University, Faculty of Medicine, Ocular Surface Research Laboratory, Izmir, Turkey
[h] Ege University Technopark, Limbustem R&D Medical Products Ltd., Izmir, Turkey
[i] Ege University, Department of Stem Cell, Institute of Health Sciences, Izmir, Turkey
[j] Ege University, Cord Blood Cell-Tissue Application and Research Center, Izmir, Turkey

ARTICLE INFO

Keywords:
Topical insulin
Corneal chemical burn
Telocyte-like cells
Stromal remodeling

ABSTRACT

Aim: This study aimed to investigate the regenerative efficacy of topically administered insulin on corneal epithelial and stromal healing in a well-established rabbit model of ocular surface damage induced by chemical injury.

Methods: A standardized alkali burn model was created in the right eyes of 16 New Zealand white rabbits. Animals were randomly assigned into four groups: insulin-treated group (I group, n = 6), polyvinyl alcohol + povidone-treated group (P group, n = 6), untreated control group (C group, n = 4), and uninjured healthy controls (H group, n = 3).

Results: No statistically significant differences were observed among experimental groups regarding the epithelial defect area on day 1. By day 3, complete epithelial closure was achieved in all treated groups. There was no major intergroup differences were observed in surface integrity or clarity; in fact, insulin did not enhance epithelial healing or improve clinical scores compared to the control group However, stromal edema persisted more prominently in the insulin and control groups compared to healthy controls. Although α-SMA immunoreactivity did not show a significant intergroup difference, its relative increase in the insulin group may reflect early fibrotic remodeling. Electron microscopy demonstrated more compact and aligned collagen fibrils, as well as a greater density of telocyte-like interstitial cells in the insulin group—suggestive of enhanced stromal restructuring and repair.

Discussion: Topical insülin was associated with ultrastructural changes suggestive of stromal remodeling following chemical injury, although histological findings (including marked stromal edema) and the absence of clinical improvement indicate that its effect on overall corneal restoration remains uncertain. The presence of telocyte-like cells and improved collagen fibril organization in the insulin-treated corneas indicates a potential role for insulin in promoting physiological stromal remodeling. These findings support further investigation into insulin-based topical therapies for corneal wound healing.

1. Introduction

Chemical eye injuries represent true ophthalmic emergencies, with outcomes ranging from transient epithelial defects to irreversible visual loss (Haring et al., 2016). Among these, alkali burns are particularly devastating due to their rapid tissue penetration and profound cytotoxicity, leading to persistent epithelial defects, ocular surface inflammation, reduced tear secretion, enhanced proteolytic activity, oxidative

* Corresponding author. Balıkesir University, Faculty of Medicine, Department of Ophthalmology, Balıkesir, Turkey.
E-mail address: gozdejcgrl@gmail.com (G.S. Vural).

https://doi.org/10.1016/j.exer.2025.110775
Received 8 August 2025; Received in revised form 11 November 2025; Accepted 25 November 2025
Available online 26 November 2025

stress, decreased corneal innervation, and impaired collagen remodeling. These pathophysiological cascades often culminate in sterile stromal ulceration, neovascularization, corneal opacification, and, in severe cases, globe perforation and loss (Wagoner, 1997). Despite the use of standard protocols and current therapeutic modalities, outcomes remain suboptimal in many cases (Brodovsky et al., 2000).

The ophthalmic application of insulin was first introduced in 1945 (Aynsley, 1945), paving the way for investigations into its therapeutic potential in ocular surface disorders (Bastion and Ling, 2013; Diaz-Valle et al., 2021; Jaworski et al., 2023). Topical insulin has demonstrated efficacy in treating persistent epithelial defects (PED), neurotrophic keratopathy, dry eye disease, and diabetic keratopathy (Burgos-Blasco et al., 2024; Dasrilsyah et al., 2023; Diaz-Valle et al., 2022; Jaworski et al., 2023). Experimental and clinical studies have shown that insulin stimulates corneal epithelial proliferation and migration, enhances epithelial barrier function, and accelerates healing. These effects are mediated through mechanisms such as stimulation of DNA synthesis, inhibition of apoptosis via the PI3K/Akt/mTOR pathway, suppression of pro-inflammatory cytokines, and improved mitochondrial respiration (Stuard et al., 2020).

The interactions of insulin with extracellular matrix (ECM) components in extraocular tissues have been demonstrated through experimental and clinical studies. Insulin has been reported to enhance protein synthesis in cardiac myocytes, stimulate DNA synthesis in fibroblasts, promote fibroblast migration and differentiation, and accelerate wound healing by increasing collagen deposition and ECM formation (Khattab et al., 2025; Tokudome et al., 2004; Wang and Xu, 2020).

However, despite promising evidence in metabolic and neurotrophic corneal disorders, there remains a notable paucity of data regarding its utility in acute chemical burns.

In this study, we aimed to assess the therapeutic efficacy of topical insulin in a rabbit model of chemical burn-induced ocular surface injury. A comprehensive multimodal analysis—including clinical observation, histopathology, α-smooth muscle actin (α-SMA) immunohistochemistry, and ultrastructural evaluation via electron microscopy—was employed to investigate insulin's impact on corneal epithelial regeneration and, in particular, stromal remodeling.

2. Materials and methods

2.1. Study design and ethical compliance

This experimental study was conducted through a collaborative effort between three academic institutions: the experimental modeling, animal care, and corneal tissue harvesting were carried out at the Laboratory Animal Application and Research Center of Ege University (EGEHAYMER); histopathological and immunohistochemical analyses were conducted at the Department of Histology and Embryology, Faculty of Medicine, Balıkesir University; and ultrastructural evaluations via electron microscopy were performed at the Department of Histology and Embryology, Cerrahpaşa Faculty of Medicine, Istanbul University-Cerrahpaşa. All procedures involving animals were conducted in accordance with the regulation for the ethical conduct of animal research and institutional guidelines.

2.2. Experimental model

A total of 16 healthy New Zealand albino rabbits (5–6 months old, 1500–2000 g) of both sexes were used in our study. The experimental rabbits were obtained from EGEHAYMER and housed in specially designed rabbit cages at this center, where they were provided with sufficient water and feed appropriate for their physiology, and kept at a controlled temperature (21.0 ± 2 °C) and humidity level. The rabbits were quarantined for 20 days before being included in the study.

To induce general anesthesia in rabbits, 35–50 mg/kg ketamine hydrochloride (Ketasol 10 %, Richter Pharma, Austria) and 5–10 mg/kg xylazine hydrochloride (Sanalazin 20, Santavet, Turkey) was administered intramuscularly to induce general anesthesia in rabbits, followed by topical application of 0.5 % proparacaine hydrochloride (Alcaine® ophthalmic solution, Alcon-Couvreur, Belgium). An alkaline burn model was created in the right eyes of the rabbits, while no procedure was performed on the left eyes.

To create the chemical burn, 1N NAOH-soaked sponges measuring 8 mm × 2 mm, cut at the ends and prepared, were applied to the central area of the cornea of the right eye, which was placed in the blepharostat, for 30 s. The ocular surface was then rinsed with isotonic solution [0.9 % sodium chloride (NaCl)) for 2 min. One rabbit in the insulin group was excluded from the study because the chemical burn model came into contact with the limbus during its creation.

After the experimental model was established, the rabbits were randomized into three groups. Four rabbits were assigned to the control group, and six rabbits were assigned to each of the other two groups. To minimize the number of subjects, one rabbit from each group was randomly selected, and its left eye was used as the healthy group, as detailed in the following group descriptions.

Healthy group (H group): The left eye of rabbits that did not undergo any treatment was taken as the healthy group.

Control group (C group): One drop of normal saline was instilled into the right eye four times a day (at 08:00, 12:00, 16:00, and 18:00) for 28 days.

Polyvinyl alcohol + Povidone group (P group): One drop of polyvinyl alcohol and povidone (Novaqua 0.4 ml vial eye drops, 5.60 mg polyvinyl alcohol and 2.40 mg povidone, Deva, Istanbul, Turkey) was instilled into the right eye four times a day (at 08:00, 12:00, 16:00, and 18:00) for 28 days.

Insulin group (I group): One drop of insulin (Humulin N 100 IU/ml 10 ml vial, Eli Lilly and Company, Indianapolis/Indiana/USA, 1 IU/mL concentration, diluted in polyvinyl alcohol and povidone) was instilled into the right eye four times a day (at 08:00, 12:00, 16:00, and 18:00) for 28 days.

C group and P group were included to distinguish the potential effects of the vehicle from those of insulin itself. The normal saline group (C) served as a baseline control, while the artificial tear solution group (P) was used as a vehicle control corresponding to the solvent used for insulin preparation.

Topical moxifloxacin (Moxai 0.5 % eye drops, Abdi İbrahim, Turkey) was applied to prevent infection while the epithelium remained open.

In our study, insulin was prepared at a concentration of 1 IU/ml by diluting the vial form of insulin for subcutaneous injection in polyvinyl alcohol and povidone (Burgos-Blasco et al., 2024). The drops were prepared under sterile conditions in sterile containers and stored in a refrigerator. The prepared insulin solutions were used for one week. New drops were prepared each week.

After the chemical burn model was created, examinations were performed on days 1, 3, 5, 7, 14, 21, and 28.

Clinical examinations were conducted without prior knowledge of the treatment allocation to minimize observer bias. All histological and immunohistochemical evaluations were also performed by an experienced pathologist who was blinded to the group assignments.

During visits, the clinical condition of the subjects and the size of the epithelial defect were recorded by photographing them. Three parameters were used to evaluate the clinical condition: chemosis, conjunctival hyperemia, and eyelid edema. These three parameters were scored on a scale of 0–3 and recorded (Sotozono et al., 2007). Epithelial defect areas were measured using ImageJ (National Institutes of Health, Bethesda, MD, Wayne Rasband at Research Services Branch) (Fig. 1).

The rabbits were sacrificed using high-dose im ketamine hydrochloride (Ketasol 10 %, Richter Pharma, Austria) and xylazine hydrochloride (Sanalazin 20, Santavet, Turkey) on day 28. After sacrifice, the cornea was dissected 1 mm behind the limbus. From each group, corneal tissue was excised using a 4 mm punch from two randomly selected rabbits, passing through the site of chemical burn, for electron

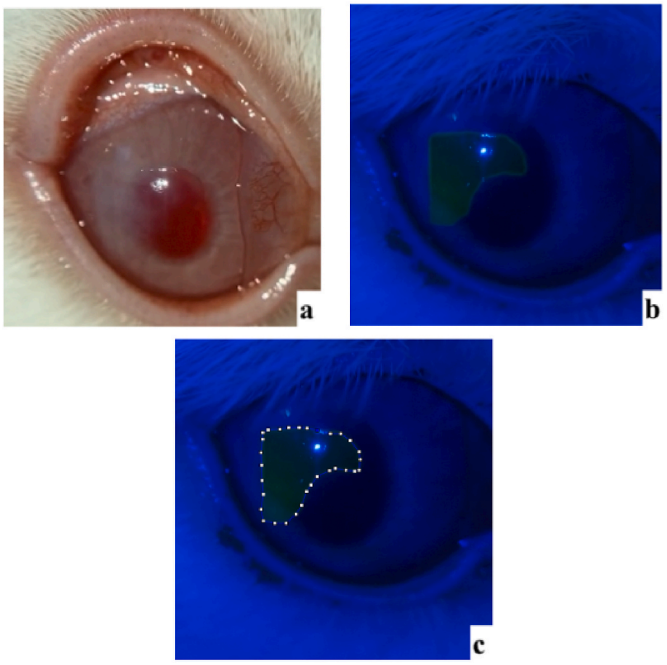

Fig. 1. Images of the created chemical burn model.
The photo of the rabbit with the chemical burn model on the first day of the first visit is shown in Fig. 1a, the photo taken under cobalt blue with fluorescein drops is shown in Fig. 1b, and the photo with the epithelial defect measurement performed in the ImageJ program is shown in Fig. 1c. (For interpretation of the references to colour in this figure legend, the reader is referred to the Web version of this article.)

microscopy. Tissue obtained for light microscopic analysis was fixed with 10 % neutral buffered formalin solution, while tissue obtained for electron microscopic analysis was fixed with 2.5 % glutaraldehyde.

2.3. Histological and immunohistochemical analysis

The fixed tissues were then dehydrated using a series of ascending alcohol concentrations. After clearing with toluene, they were embedded in paraffin blocks. Sections of 5 μm were taken from the prepared paraffin blocks. These sections were stained with hematoxylin and eosin (H&E) for histological examination. During the staining process, the sections were first stained with hematoxylin for 20 min, followed by bluing with tap water for 15 min. Excess stain was removed with acid alcohol, and a second bluing step was performed. The sections were then stained with eosin. Finally, the slides were dehydrated through a series of ascending alcohols and cleared with toluene. As a result of this staining, the nuclei were stained purple and the cytoplasm was stained pink. The H&E-stained sections were examined under an Olympus BX53 light microscope (Olympus, Tokyo, Japan) and photographed with a DP73 camera (Olympus, Tokyo, Japan). The samples were evaluated for stromal edema, epithelial damage, vascularization, and lymphatic infiltration parameters and scored semi-quantitatively. Scoring was performed as follows: 0 = none, 1 = low level, 2 = moderate level, 3 = high level.

For the immunohistochemical evaluation of the wound healing process in corneal sections, α-SMA labeling, a myofibroblast marker, was performed. All sections were examined Olympus BX53 light microscope (Olympus, Tokyo, Japan) and photographed with a DP73 camera (Olympus, Tokyo, Japan). For evaluation, an average of three sections were examined from corneal tissue sections obtained from each rabbit, and the percentage of the area showing α-SMA positivity within the total stromal area was calculated using the Image J program (National Institutes of Health, Bethesda, MD, Wayne Rasband at Research Services Branch) to obtain the average values for each group. Immunohistochemistry was performed using the following method (Güvenç et al., 2025): 5 μm sections were taken from paraffin-embedded corneal blocks onto adhesive slides and left in a 56 °C oven before the paraffin was removed in toluene. The sections were passed through a series of decreasing alcohol concentrations and then placed in distilled water. The sections were washed in phosphate-buffered saline (PBS) and then treated with 3 % H_2O_2 for 10 min to stop endogenous peroxidase activity. After 3 × 5 min of PBS washing, the sections were incubated in blocking solution (Thermo Scientific TP-125-HL, USA) for 5 min to prevent non-specific antibody binding. Following blocking, the sections were incubated overnight at +4 °C with anti-α-SMA antibody (A2547, Sigma Aldrich, USA) at a 1:200 dilution Then incubation, the sections were washed with PBS for 3 × 5 min and then incubated in a biotinylated secondary antibody solution (Thermo Scientific TP-125-HL, USA) for 10 min. After washing with PBS for 3 × 5 min, the sections were incubated in streptavidin peroxidase solution (Thermo Scientific TP-125-HL, USA) for 10 min. Following washing with PBS for 3 × 5 min, aminoethyl carbazole (AEC) chromogen (Thermo Scientific TA-125-HA, USA) was applied to the sections. Then the reaction had finished, the sections were placed in distilled water and sealed.

2.4. Transmission electron microscopy analysis

The fixed tissues were washed with 0.1 M phosphate buffer. The washed samples were subjected to secondary fixation in a 1 % osmium tetroxide solution at +4 °C for 1 h. Following washing with phosphate buffer, the samples were dehydrated by incubating them for 10 min each in a series of alcohol solutions at 30 %, 50 %, 70 %, 80 %, 96 %, and 100 %. They were blocked in pure propylene for 2 × 10 min and in propylene-araldite mixtures [(propylene oxide:araldite (1:1), propylene oxide:araldite (1:3), and pure araldite]. After being kept at room temperature for 1 h, they were polymerized in an araldite capsule at 60 °C in an oven for 18 h to form blocks. The resulting blocks were shaved using a trimming device. After obtaining the cross-sectional surface, semi-thin sections 0.5 μm thick were taken for region identification. Ultra-thin sections, 40–60 nm thick, were taken on copper grids. The sections were contrasted by incubating them on uranyl acetate and lead citrate drops for 45 min and 15 min, respectively, and then examined under a Jeol JEM-1011 transmission electron microscope (TEM). The examined areas were photographed using an Olympus Soft Imaging camera system.

2.5. Statistical analysis

SPSS version 21.0 statistical software was used for statistical analyses. The Shapiro-Wilk normality test was used to assess whether the data belonging to the groups were normally distributed. Since the histological data did not follow a normal distribution and the sample sizes were small, the significance between groups was evaluated using the nonparametric Kruskal-Wallis test. When analyzing the examination data, the one-way ANOVA test was used to compare quantitative values between groups for data that followed a normal distribution, and the Kruskal-Wallis test was used for data that did not follow a normal distribution. The Paired Sample-t test was used to evaluate changes in quantitative values between visits. The Chi-square test was used to compare qualitative values between groups and between visits. A p-value below 0.05 was considered statistically significant.

3. Results

3.1. Biomicroscopic findings

Following the induction of the chemical burn model on day 0, a total of seven follow-up visits were conducted on days 1, 3, 5, 7, 14, 21, and 28. During each visit, anterior segment photographs were taken, and the

epithelial defect area was assessed using fluorescein staining.

On day 1, there was no statistically significant difference in the epithelial defect area among the groups ($p = 0.683$). By day 3, complete epithelial closure was observed in all rabbits.

Clinical parameters including chemosis, conjunctival hyperemia, and eyelid edema were also evaluated on days 1, 3, and 5. Statistical analysis revealed no significant differences between the groups for any of these parameters (chemosis: day 1 $p = 0.318$, day 3 $p = 0.880$, day 5 $p = 0.523$; conjunctival hyperemia: day 1 $p = 0.318$, day 3 $p = 0.448$, day 5 $p = 0.880$; eyelid edema: day 1 $p = 0.343$, day 3 $p = 0.566$).

Clinically, eyelid edema resolved completely by day 3 in all groups. Similarly, chemosis was no longer evident by day 7, and conjunctival hyperemia—initially mild—resolved entirely by the subsequent visit (Tables 1–3).

3.2. Histological findings

Corneal tissues were evaluated based on stromal edema, epithelial damage, vascularization, and lymphatic infiltration parameters. Semi-quantitative scoring data for each group are presented in Table 4. According to these data, epithelial damage and stromal edema increased significantly in all groups compared to group H. The highest vascularization was present in the stromal area immediately below the anterior surface epithelium in the C group, and the treatments reduced vascularization. Lymphatic infiltration was elevated in all groups compared to the H group. Additionally, in some samples, collagen organization in the stroma of the wound healing areas was observed to be disrupted.

Statistical evaluation of the results showed that there was a significant difference between the groups in terms of stromal edema and epithelial damage (p = 0.021, p = 0.027, respectively), while no statistical significance was observed in terms of vascularization and lymphatic infiltration. When evaluated for stromal edema, the groups that showed statistical significance were the H and C groups (p = 0.017) and the H and I groups (p = 0.003). For epithelial damage, pairwise comparisons revealed significance originating from the H and C groups (p = 0.017), H and P groups (p = 0.002), and H and I groups (p = 0.019). H&E stains for the groups are shown in Fig. 2.

Table 1
Distribution of chemosis scores percentages and p values in various visits for groups.

	CONTROL (%) N = 4	GROUP P (%) N = 6	GROUP I (%) N = 6	P value
CHEMOSİS (%)				
DAY 1				
• **NO FINDING**	0	0	0	0,318
• **MILD**	100	83,3	60	
• **MODERATE**	0	16,6	40	
• **SEVERE**	0	0	0	
DAY 3				
• **NO FINDING**	25	33,3	20	0,880
• **MILD**	75	66,6	80	
• **MODERATE**	0	0	0	
• **SEVERE**	0	0	0	
DAY 5				
• **NO FINDING**	75	83,3	100	0,523
• **MILD**	25	16,6	0	
• **MODERATE**	0	0	0	
• **SEVERE**	0	0	0	
DAY 7				
• **NO FINDING**	100	100	100	–
• **MILD**	0	0	0	
• **MODERATE**	0	0	0	
• **SEVERE**	0	0	0	

Table 2
Distribution of conjunctival hyperemia scores percentages and p values in various visits for groups.

	CONTROL (%) N = 4	GROUP P (%) N = 6	GROUP I (%) N = 6	P value
CONJUNCTIVAL HYPEREMIA (%)				
DAY 1				
• **NO FINDING**	0	0	0	0,318
• **MİLD**	0	0	0	
• **MODERATE**	100	83,3	60	
• **SEVERE**	0	16,6	40	
DAY 3				
• **NO FINDING**	0	0	0	0,448
• **MILD**	0	16,6	0	
• **MODERATE**	100	83,3	100	
• **SEVERE**		0	0	
DAY 5				
• **NO FINDING**	0	0	0	0,880
• **MILD**	75	66,6	80	
• **MODERATE**	25	33,3	20	
• **SEVERE**	0	0	0	
DAY 7				
• **NO FINDING**	0	0	0	0,448
• **MILD**	50	83,3	100	
• **MODERATE**	50	16,6	0	
• **SEVERE**	0	0	0	

Table 3
Distribution of eyelid edema scores percentages and p values in various visits for groups.

	CONTROL (%) N = 4	GROUP P (%) N = 6	GROUP I (%) N = 6	P value
EYELID EDEMA (%)				
DAY 1				
• **NO FINDING**	0	83,3	0	0,343
• **MILD**	100	16,6	80	
• **MODERATE**	0	0	20	
• **SEVERE**	0	0	0	
DAY 3				
• **NO FINDING**	75	50	40	0,566
• **MILD**	25	50	60	
• **MODERATE**	0	0	0	
• **SEVERE**	0	0	0	
DAY 5				
• **NO FINDING**	100	100	100	–
• **MILD**	0	0	0	
• **MODERATE**	0	0	0	
• **SEVERE**	0	0	0	
DAY 7				
• **NO FINDING**	%100	%100	%100	–
• **MILD**	%0	%0	%0	
• **MODERATE**	%0	%0	%0	
• **SEVERE**	%0	%0	%0	

3.3. Immunohistochemical findings

Immunohistochemical staining for α-SMA, a myofibroblast marker, revealed that the proportion of α-SMA-positive areas in the stroma was 2.873 % in the H group (95 % CI: 2.60–3.14), 2.724 % in the C group (95 % CI: 0.12-5.57), 1.861 % in the P group (95 % CI: 0.23–3.69), and 4.771 % in the I group (95 % CI: 2.78–6.76). A relative decrease was observed in the P group compared to the H and C groups, while an increase was determined in the I group. No statistical significance was observed between the groups (p = 0.093). Micrographs related to

Table 4
Histological examination data.

	Stromal Edema	Epithelial Disruption	Vascularization	Lymphatic Infiltration
H	0	0	0	0
C	2,25 ± 0,25	2,25 ± 0,25	1 ± 0,7	1 ± 0,7
P	1,8 ± 0,37	2,2 ± 0,20	0,4 ± 0,24	1,2 ± 0,5
I	2,6 ± 0,24	2 ± 0,32	0,4 ± 0,4	1,8 ± 0,4
p value	[a]**0,021**	[a]**0,027**	p = 0,513	p = 0,085

Group H: Healthy Group, Group C: Control Group, Group P: Polyvinyl alcohol + Povidone Group, Group I: Insulin Group.
p value: statistical significance value.
[a] Statistically significant Value.

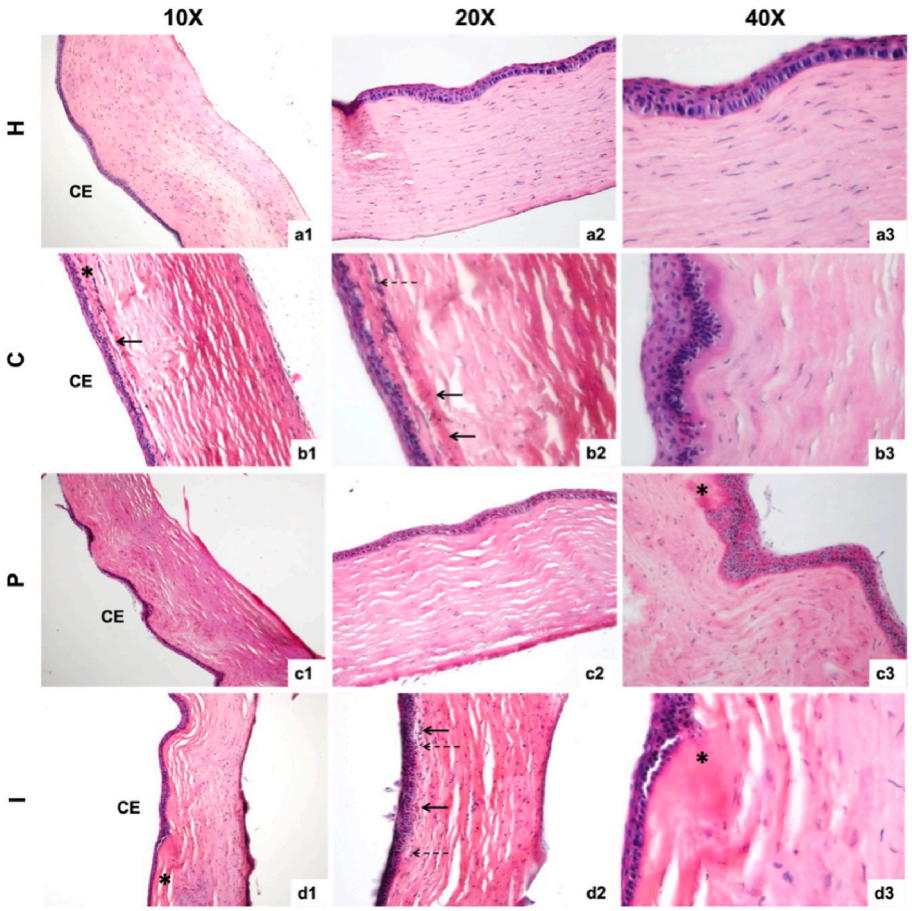

Fig. 2. Corneal micrographs of groups.
(a1-a3): Group H, (b1-b3): Group C, (c1-c3): Group P, (d1-d3): Group I.
CE: Corneal epithelium, black arrow: vascularization, dashed arrow: lymphatic infiltration, asterisk: disruption of collagen arrangement in the stroma.
Hematoxylin and eosin, 10x, 20x, 40x

immunohistochemical analyses and the expression rate graph for the groups are presented in Fig. 3.

3.4. Electron microscopic findings

The corneal stroma region, which appeared normally organized in healthy rabbits (Fig. 4a), showed irregular and sparse collagen organization in the C group, and the frequency of fibers had decreased (Fig. 4b). When the stroma of the treatment groups was examined, it was observed that the collagen fibers in the I group (Fig. 4c) were more regularly arranged than those in the P group (Fig. 4d).

Additionally, in the insulin group, telocyte-like cells, which are known to play an important role in tissue regeneration and repair in the stromal area and are characterized by long, thin extensions, were observed (Fig. 5-a-c).

4. Discussion

In this experimental rabbit model of ocular surface injury induced by chemical burns, no statistically significant differences were observed among the treatment groups in terms of epithelial healing, clinical scores, or α-smooth muscle actin (α-SMA) immunoreactivity. Nevertheless, ultrastructural analysis via transmission electron microscopy (TEM) demonstrated more organized collagen fibril architecture in the insulin-treated group. Additionally, telocyte-like interstitial cells—recognized for their regulatory roles in tissue renewal and regeneration—were observed in the stromal compartment of this group. Histological analysis confirmed increased epithelial damage in all experimental groups compared to healthy controls, with pronounced stromal edema evident in both the insulin and control groups.

Epithelial defect size and the duration of re-epithelialization are

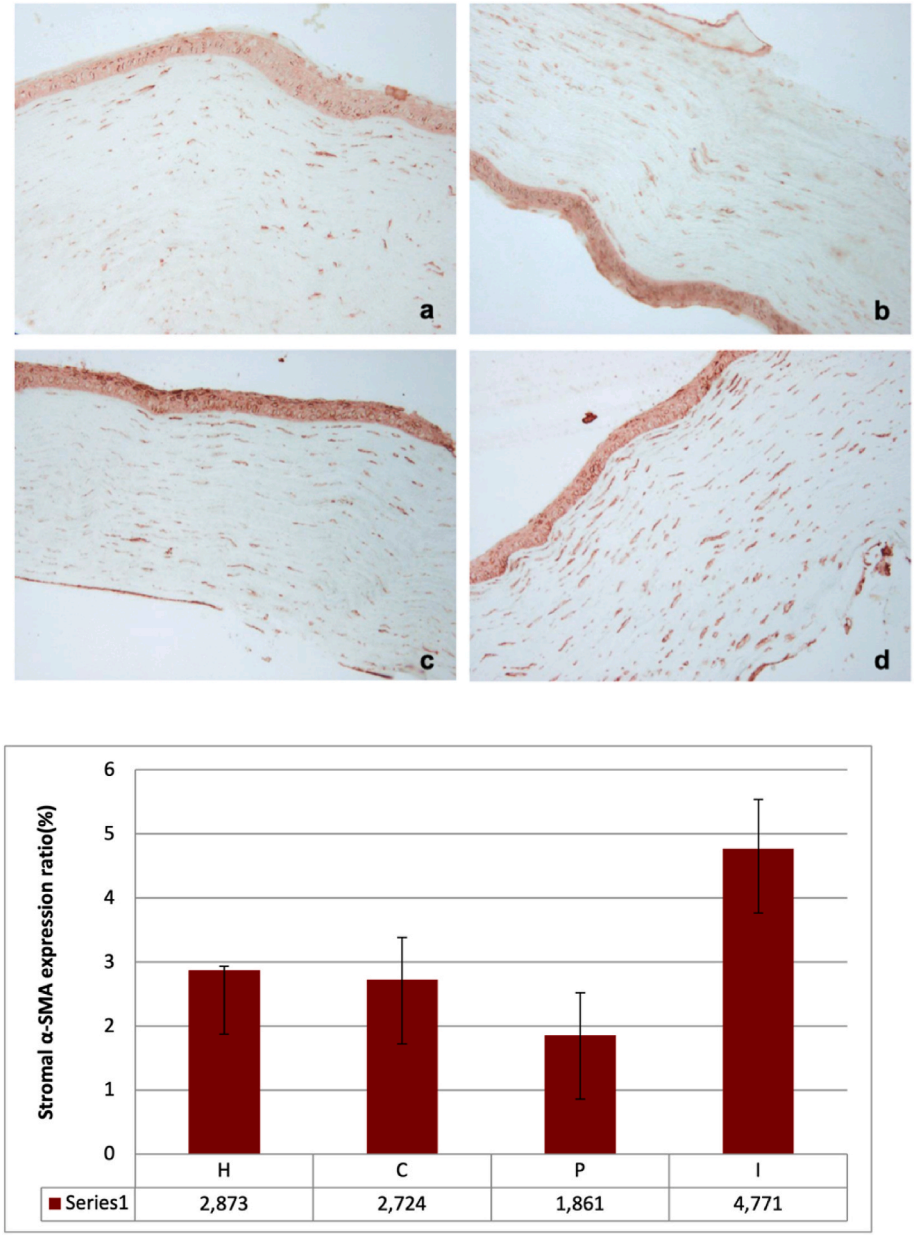

Fig. 3. Immunohistochemical Analyses of α-SMA Marker.
a: Group H, b: Group C, c: Group P, d: Group I, f: Percentage of α-SMA-positive areas in the stroma.

critical prognostic markers in the clinical management of chemical ocular burns. These parameters are influenced by multiple variables, including the integrity of the limbal stem cell niche, degree of neurotrophic dysfunction, severity of inflammation, presence of infection, and adherence to therapeutic regimens. In the acute phase, chemical insult triggers a robust inflammatory cascade involving pro-inflammatory cytokines, interleukins, reactive oxygen species, and neutrophils, all of which compromise stromal homeostasis and may impede epithelial regeneration, predisposing the cornea to persistent epithelial defects, ulceration, or even perforation (Ghiasi et al., 2018).

In our study, the initial epithelial defect areas were comparable across all groups on day 1, indicating successful randomization and standardization. Complete re-epithelialization was observed by day 3 in all experimental groups (C, P, and I), consistent with prior reports (Zhang et al., 2018). The complete epithelial closure was achieved by day 3 in all groups, including the untreated control, suggests that the chemical injury model used in this study was relatively mild. Consequently, the ability to detect a potential therapeutic effect of insulin on epithelial healing may have been limited; however, this effect has been observed more prominently in previous studies employing more severe or diabetic models. For instance, Fai et al. reported that topical insulin in saline promoted faster epithelial closure compared to saline alone in diabetic patients undergoing vitrectomy with corneal debridement (Fai et al., 2017). Other studies also found that insulin outperformed sodium hyaluronate in enhancing epithelial repair (Dasrilsyah et al., 2023; Quiroz-Mendoza et al., 2021). These effects are mechanistically linked to insulin's ability to stimulate DNA synthesis, inhibit autophagy through the PI3K/Akt/mTOR pathway, downregulate inflammatory mediators, and promote mitochondrial function (Stuard et al., 2020).

Histological assessment further revealed significantly greater epithelial damage and stromal edema in all experimental groups relative to the healthy controls. Of note, the most pronounced stromal edema was observed in the insulin and control groups. Interestingly, despite full

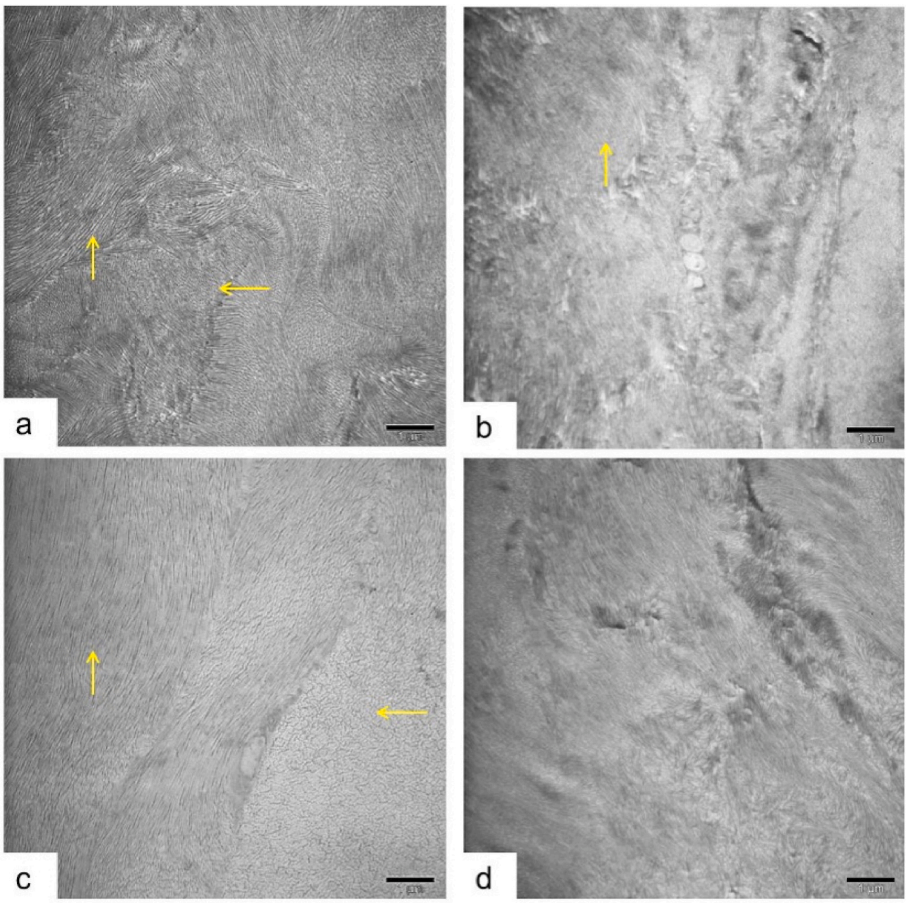

Fig. 4. Electron microscopy images.
a: Healthy, b: Control, c: Group I, d: Group P. Arrows: Cross-sectional and longitudinal collagen fiber sections.

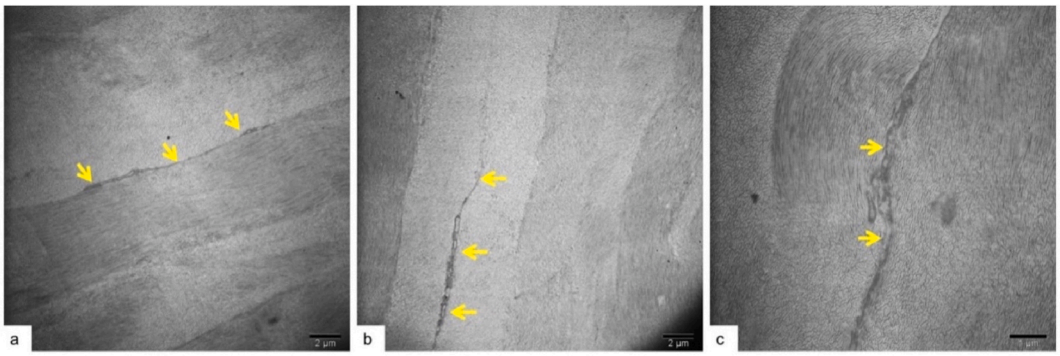

Fig. 5. Electron microscopy images of the insulin group.
Arrows: Telocyte-like cells.

epithelial closure by day 3, histopathological signs of epithelial disruption persisted at day 28, underscoring the discrepancy between clinical re-epithelialization and true histological recovery. Restoration of epithelial integrity and homeostasis involves not only epithelial resurfacing but also a functional tear film and sustained metabolic support. Given its capacity to enhance mitochondrial respiration and cellular proliferation, insulin may provide such support. Although not statistically significant, a downward trend in epithelial damage in the insulin group suggests that topical insulin may contribute to improved epithelial resilience over time. Despite showing the highest degree of stromal edema histologically, the insulin-treated corneas exhibited the most organized collagen fibril architecture ultrastructurally. This apparent discrepancy may reflect insulin-induced alterations in stromal hydration or edema composition rather than true structural deterioration. However, this interpretation remains speculative and warrants further investigation.

Immunohistochemical evaluation of α-SMA—a marker of myofibroblast differentiation—revealed a relative increase in expression in the insulin group. Myofibroblasts are key mediators of stromal repair, synthesizing extracellular matrix components and collagen to facilitate wound closure and mechanical stability. However, excessive or prolonged activation of myofibroblasts is known to be associated with stromal fibrosis or delayed healing (Wilson, 2012). Peterson et al. reported increased α-SMA levels in the corneas of insulin-treated diabetic

patients and canines, raising the possibility that insulin influences keratocyte-to-myofibroblast transdifferentiation (Peterson and Chandler, 2022). Further studies are warranted to delineate insulin's role in myofibroblast regulation and fibrotic remodeling.

TEM analysis revealed superior collagen organization in the insulin group, along with the presence of telocyte-like cells—novel interstitial cells characterized by their long cytoplasmic extensions (telopodes) and first described by Popescu et al., in 2010 (Popescu and Faussone-Pellegrini, 2010). These cells establish three-dimensional stromal networks via homo- and heterocellular junctions with resident cell populations including stem cells, fibroblasts, melanocytes, macrophages, nerve terminals, and vascular structures (Bei et al., 2015; Luesma et al., 2013; Marini et al., 2017; Petrea et al., 2018; Popescu and Faussone-Pellegrini, 2010; Semiz et al., 2022). Telocytes have been implicated in intercellular communication through release of extracellular vesicles (e.g., exosomes) and are thought to contribute to tissue homeostasis, particularly in the context of regeneration and repair. Marini et al. showed that telocytes in keratoconus corneas exhibit mitochondrial dysfunction and impaired gap junction formation, suggesting their importance in maintaining stromal integrity. To our knowledge, this is the first study to demonstrate telocyte-like cells in chemically injured corneas treated with topical insulin. Their co-localization with organized collagen fibrils and α-SMA-positive cells implies a role in regenerative stromal remodeling potentially enhanced by insulin exposure.

The present findings indicate a potential association between insulin treatment and the presence of telocyte-like cells within the corneal stroma. Insulin may support telocyte survival or activity, thereby contributing to stromal remodeling and repair. However, this proposed interaction remains hypothetical and requires further mechanistic investigation to be confirmed.

The absence of a measurable effect of insulin on epithelial healing in this model may be attributed to several factors. The animals used were non-diabetic, and the chemical injury was relatively mild, sparing the limbal region. These conditions likely minimized the regenerative challenge, thereby reducing the potential for insulin to exert a detectable therapeutic benefit. This context may explain the discrepancy between the present findings and previous reports showing enhanced epithelial healing with topical insulin in more severe or diabetic models.

This study has several limitations. A major limitation of this study is the small sample size, which likely reduced the statistical power to detect significant differences in certain parameters, such as α-SMA immunoreactivity and histological scores. Short follow-up period may have limited our ability to detect subtler differences, particularly in epithelial recovery and immune responses. The two-day visit intervals during the first week precluded finer resolution of early epithelial healing dynamics. Moreover, the mild chemical injury model used here may restrict the generalizability of these findings to more severe burn scenarios. Finally, the observed association between insulin treatment and telocyte-like cells should be interpreted as correlative rather than causal.Future studies should incorporate more severe burn models, include daily monitoring in the acute phase, and specifically investigate insulin's role in modulating limbal stem cell regeneration and preventing long-term fibrotic outcomes.

5. Conclusion

In conclusion, while topical insulin did not produce a significant improvement in epithelial or clinical outcomes in this mild chemical injury model, it was associated with promising ultrastructural findings indicative of enhanced stromal remodeling. Given that stromal healing is a protracted and complex process—often spanning 6–12 months depending on the depth and severity of the insult—early intervention with insulin may offer dual-phase benefits: accelerating initial wound resolution and enhancing long-term tissue homeostasis.

To our knowledge, this is the first study to investigate the ultrastructural impact of topical insulin on corneal stromal regeneration using transmission electron microscopy. The observed presence of telocyte-like cells and improved collagen alignment underscore insulin's putative role as a bioactive modulator of stromal repair. These preliminary findings provide compelling rationale for further investigation. Future studies employing larger sample sizes, extended observation periods, and molecular profiling are warranted to elucidate the mechanisms by which insulin influences stromal remodeling, myofibroblast activation, and extracellular matrix organization in the context of ocular surface injury. Moreover, investigating these effects in the context of dry eye disease and ocular surface reconstruction may provide novel therapeutic insights.

CRediT authorship contribution statement

Yurdagul Girgin: Writing – review & editing, Writing – original draft, Visualization, Validation, Supervision, Software, Resources, Project administration, Methodology, Investigation, Formal analysis, Data curation, Conceptualization. **Gozde Sahin Vural:** Writing – review & editing, Writing – original draft, Validation, Supervision, Software, Resources, Project administration, Methodology, Investigation, Funding acquisition, Formal analysis, Conceptualization. **Yucel Yigit:** Writing – review & editing, Writing – original draft, Methodology, Data curation, Conceptualization. **Basak Isildar:** Writing – review & editing, Writing – original draft, Visualization, Validation, Methodology, Data curation. **Pakize Nur Akkaya:** Writing – review & editing, Writing – original draft, Methodology, Formal analysis. **Gamze Tanriverdi:** Visualization, Validation, Supervision, Methodology, Data curation. **Muhammed Dara Tas:** Writing – review & editing, Data curation, Conceptualization. **Ozlem Barut Selver:** Writing – review & editing, Writing – original draft, Visualization, Validation, Supervision, Methodology, Data curation, Conceptualization.

Conflict of interest

The authors declare that they have no known competing financial interests or personal relationships that could have appeared to influence the work reported in this paper.

Acknowledgement

This research was funded by the Balikesir University Scientific Research Project Foundation (BAP No: 2023/081) and Balikesir University Foundation.

Data availability

Data will be made available on request.

References

Aynsley, T.R., 1945. The use of insulin in the treatment of corneal ulcers. Br. J. Ophthalmol. 29, 361–363. https://doi.org/10.1136/bjo.29.7.361.

Bastion, M.C., Ling, K., 2013. Topical insulin for healing of diabetic epithelial defects. In: A retrospective review of corneal debridement during vitreoretinal surgery in Malaysian patients history indication date of procedure, 68, pp. 208–216.

Bei, Y., Wang, F., Yang, C., Xiao, J., 2015. Telocytes in regenerative medicine. J. Cell Mol. Med. 19, 1441. https://doi.org/10.1111/JCMM.12594.

Brodovsky, S.C., McCarty, C.A., Snibson, G., Loughnan, M., Sullivan, L., Daniell, M., Taylor, H.R., 2000. Management of alkali burns : an 11-year retrospective review. Ophthalmology 107, 1829–1835. https://doi.org/10.1016/S0161-6420(00)00289-X.

Burgos-Blasco, B., Diaz-Valle, D., Rego-Lorca, D., Perez-Garcia, P., Puebla-Garcia, V., Fernandez-Vigo, J.I., Benitez-del-Castillo, J.M., Gegundez-Fernandez, J.A., 2024. Topical insulin, a novel corneal epithelial regeneration agent in dry eye disease. Eur. J. Ophthalmol. 34, 719–725. https://doi.org/10.1177/11206721231206790.

Dasrilsyah, A.M., Wan Abdul Halim, W.H., Mustapha, M., Tang, S.F., Kaur, B., Ong, E.Y., Catherine Bastion, M.L., 2023. Randomized clinical trial of topical insulin versus artificial tears for healing rates of iatrogenic corneal epithelial defects induced

during vitreoretinal surgery in diabetics. Cornea 42, 1395–1403. https://doi.org/10.1097/ICO.0000000000003308.
Diaz-Valle, D., Burgos-Blasco, B., Gegundez-Fernandez, J.A., Garcia-Caride, S., Puebla-Garcia, V., Peña-Urbina, P., Benitez-del-Castillo, J.M., 2021. Topical insulin for refractory persistent corneal epithelial defects. Eur. J. Ophthalmol. 31, 2280–2286. https://doi.org/10.1177/1120672120958307.
Diaz-Valle, D., Burgos-Blasco, B., Rego-Lorca, D., Puebla-Garcia, V., Perez-Garcia, P., Benitez-del-Castillo, J.M., Herrero-Vanrell, R., Vicario-de-la-Torre, M., Gegundez-Fernandez, J.A., 2022. Comparison of the efficacy of topical insulin with autologous serum eye drops in persistent epithelial defects of the cornea. Acta Ophthalmol. 100, e912–e919. https://doi.org/10.1111/aos.14997.
Fai, S., Ahem, A., Mustapha, M., Mohd Noh, U.K., Catherine Bastion, M.L., 2017. Randomized controlled trial of topical insulin for healing corneal epithelial defects induced during vitreoretinal surgery in diabetics. Asia-Pacific J. Ophthalmol. 6, 418–424. https://doi.org/10.22608/APO.201780.
Ghiasi, Z., Gray, T., Tran, P., Dubielzig, R., Murphy, C., McCartney, D.L., Reid, T.W., 2018. The effect of topical Substance-P plus Insulin-like growth Factor-1 (IGF-1) on epithelial healing after photorefractive keratectomy in rabbits. Transl. Vis. Sci. Technol. 7. https://doi.org/10.1167/TVST.7.1.12, 12–12.
Güvenç, G., Erdoğan-Öner, A., Kavak, G., Bahçeci, S.A., Kutlu, O., 2025. Effects of N-Acetylcysteine and l-Carnitine on wound healing of palatal mucosa in a rat model. J. Oral Pathol. Med. https://doi.org/10.1111/JOP.70018.
Haring, R.S., Sheffield, I.D., Channa, R., Canner, J.K., Schneider, E.B., 2016. Epidemiologic trends of chemical ocular burns in the United States. JAMA Ophthalmol. 134, 1119–1124. https://doi.org/10.1001/JAMAOPHTHALMOL.2016.2645.
Jaworski, M., Lorenc, A., Leszczyński, R., Mrukwa-Kominek, E., 2023. Topical insulin in neurotrophic keratopathy: a review of current understanding of the mechanism of action and therapeutic approach. Pharmaceutics 16. https://doi.org/10.3390/pharmaceutics16010015.
Khattab, M.A., Nabeh, O.A., Adel, S., Abdelazeem, M., Naser, M.M., Matter, L.M., 2025. Topical insulin improves postoperative wound healing in controlled diabetic patients through regulating the expression of E-Cadherin and Ki67: an open-label randomized controlled-trial. Fut. J. Pharmac. Sci. 11 (1 11), 1–12. https://doi.org/10.1186/S43094-025-00830-6, 2025.
Luesma, M.J., Gherghiceanu, M., Popescu, L.M., 2013. Telocytes and stem cells in limbus and uvea of mouse eye. J. Cell Mol. Med. 17, 1016–1024. https://doi.org/10.1111/jcmm.12111.
Marini, M., Mencucci, R., Rosa, I., Favuzza, E., Guasti, D., Ibba-Manneschi, L., Manetti, M., 2017. Telocytes in normal and keratoconic human cornea: an immunohistochemical and transmission electron microscopy study. J. Cell Mol. Med. 21, 3602–3611. https://doi.org/10.1111/jcmm.13270.
Peterson, C., Chandler, H.L., 2022. Insulin facilitates corneal wound healing in the diabetic environment through the RTK-PI3K/Akt/mTOR axis in vitro. Mol. Cell. Endocrinol. 548, 111611. https://doi.org/10.1016/j.mce.2022.111611.
Petrea, C.E., Crăiţoiu, Vrapciu, A.D., Mănoiu, V.S., Rusu, M.C., 2018. The telopode- and filopode-projecting heterogeneous stromal cells of the human sclera niche. Ann. Anat. 218, 129–140. https://doi.org/10.1016/j.aanat.2017.12.013.
Popescu, L.M., Faussone-Pellegrini, M.S., 2010. TELOCYTES - a case of serendipity: the winding way from interstitial cells of Cajal (ICC), via interstitial Cajal-like cells (ICLC) to TELOCYTES. J. Cell Mol. Med. 14, 729–740. https://doi.org/10.1111/J.1582-4934.2010.01059.X.
Quiroz-Mendoza, J.L., García-Roa, M., Romero-Morales, V., Valera-Cornejo, D., Vázquez-Membrillo, M., Ramírez-Neria, P., Villalpando-Gómez, Y., García-Franco, R., 2021. Clinical trial of topical insulin and sodium hyaluronate in the treatment of epithelial defects produced by intraoperative corneal epithelial debridement during pars plana vitrectomy in diabetics. Revista Mexicana De Oftalmología, English Edition) 95. https://doi.org/10.24875/RMOE.M21000157.
Semiz, F., Lokaj, A.S., Tanriverdi, G., Caliskan, G., Hima-Musa, N., Semiz, C.E., 2022. Fresh human myopic lenticule intrastromal implantation for keratoconus using SMILE surgery in a long-term Follow-up study: ultrastructural analysis by transmission electron microscopy. J. Refract. Surg. 38, 520–528. https://doi.org/10.3928/1081597X-20220713-02.
Sotozono, C., Ang, L.P.K., Koizumi, N., Higashihara, H., Ueta, M., Inatomi, T., Yokoi, N., Kaido, M., Dogru, M., Shimazaki, J., Tsubota, K., Yamada, M., Kinoshita, S., 2007. New grading system for the evaluation of chronic ocular manifestations in patients with Stevens-Johnson syndrome. Ophthalmology 114, 1294–1302. https://doi.org/10.1016/J.OPHTHA.2006.10.029.
Stuard, W.L., Titone, R., Robertson, D.M., 2020. The IGF/Insulin-IGFBP axis in corneal development, wound healing, and disease. Front. Endocrinol. 11, 1–15. https://doi.org/10.3389/fendo.2020.00024.
Tokudome, T., Horio, T., Yoshihara, F., Suga, S.I., Kawano, Y., Kohno, M., Kangawa, K., 2004. Direct effects of high glucose and insulin on protein synthesis in cultured cardiac myocytes and DNA and collagen synthesis in cardiac fibroblasts. Metabolism 53, 710–715. https://doi.org/10.1016/j.metabol.2004.01.006.
Wagoner, M.D., 1997. Chemical injuries of the eye: current concepts in pathophysiology and therapy. Surv. Ophthalmol. 41, 275–313. https://doi.org/10.1016/S0039-6257(96)00007-0.
Wang, J., Xu, J., 2020. Effects of topical insulin on wound healing: a review of animal and human evidences. Diabetes Metab. Syndr. Obes. 13, 719. https://doi.org/10.2147/DMSO.S237294.
Wilson, S.E., 2012. Corneal myofibroblast biology and pathobiology: generation, persistence, and transparency. Exp. Eye Res. 99, 78–88. https://doi.org/10.1016/J.EXER.2012.03.018.
Zhang, Y., Lu, X.Y., Hu, R.J., Fan, F.L., Jin, X.M., 2018. Evaluation of artificial tears on cornea epithelium healing. Int. J. Ophthalmol. 11, 1096. https://doi.org/10.18240/IJO.2018.07.04.